

Transport of Nano-C₆₀ Particles in Soil

Xuekun Cheng, Amy T. Kan, Mason B. Tomson,
Department of Civil and Environmental Engineering,
Rice University,
6100 Main Street, Houston, Texas 77005

ABSTRACT

This paper reports the first investigation of the transport of nano-C₆₀ particles (a term used to refer to underivatized C₆₀ crystalline nanoparticles, stable in water for months) through a soil column. Nano-C₆₀ particle breakthrough experiments were conducted at different flow rates. Results showed that nano-C₆₀ particles were more mobile at higher flow velocities, but exhibited only limited mobility at groundwater Darcy velocity. Spiked release of nano-C₆₀ particles occurred following flow interruption and flow velocity change. The experiment of naphthalene transport through the same soil column containing 0.18% adsorbed nano-C₆₀ particles showed that the effect of 0.18% adsorbed nano-C₆₀ particles on naphthalene transport was similar to that of 0.18% soil organic carbon.

INTRODUCTION

Nanoparticles, such as C₆₀, are expected to be manufactured in an increasing scale, meaning that they will ultimately enter the environment. The transport of those nanomaterials could possibly control their possible exposure pathways to living organisms. It has been reported that nano-C₆₀ particles are toxic to fish cells and cultured human cells^{1,2}. The public may be more concerned about the potential exposure to nano-C₆₀ particles if they are mobile in water. Since C₆₀ is virtually insoluble in water³, one might expect that this hydrophobic nanomaterial would not enter groundwater in great quantities. However, water-stable nano-C₆₀ particles can be formed in water simply by mechanical stirring, or by dissolving C₆₀ in non-polar solvents, mixing into water, followed by the removal of the solvents⁴⁻⁷, indicating that C₆₀ might be mobile in groundwater. Besides, dissolved organic matter in groundwater has been reported to significantly facilitate the transport of neutral organic contaminants⁸. The release of C₆₀ and other nanosized carbonaceous nanomaterials into aqueous environments might have similar effect. Therefore, it is of central importance to study the transport of nanomaterials in the water/sediment system, and the effect of nanomaterials on contaminant transport.

Although some work has been done to investigate C₆₀ transport through glass beads, an ideal model medium^{9,10}, the transport of C₆₀ in the natural aquatic environment may vary from that in model media due to the complicated conditions in natural soil, such as the medium heterogeneities, and the complex flow characteristics. In this work, the transport of water-stable nano-C₆₀ particles through natural soil was investigated for the first time. Breakthrough curves of nano-C₆₀ particles through a soil column was measured

at different flow rates. The transport of naphthalene through the same soil column, containing 0.18% adsorbed nano-C₆₀ particles was also measured and will be discussed.

MATERIALS AND METHODS

Materials

¹⁴C-radiolabeled naphthalene with specific activity of 6.2 μCi/μmol was purchased from Sigma-Aldrich (St. Louis, MO). A ¹⁴C-radiolabeled naphthalene stock solution with naphthalene concentration of 1129.9mg/L was prepared by diluting 100 μCi of ¹⁴C-radiolabeled naphthalene in ~1.83 mL of methanol (HPLC grade) upon receipt. Tritiated water was purchased from Amersham Co. (Arlington Hts. IL). Sodium chloride (biological grade) and sodium azide (>98%) were purchased from Fisher Scientific (Pittsburgh, PA) and Eastman Kodak Co. (Rochester, NY). Sodium azide was used to inhibit microbial activity. Toluene with a purity of 99.8% was purchased from Sigma-Aldrich. The liquid scintillation cocktail (Ready Safe™) for scintillation counting was purchased from Beckman Coulter, Inc. (Fullerton, CA).

Soil Column. Lula surface soil (92% sand, 6% silt, and 2% clay¹¹) was obtained from R.S. Kerr Environmental Research Laboratory, Ada, Oklahoma. The soil was air-dried and sieved through 10 mesh sieve and cheese cloth to remove vegetative matter. The organic carbon content of the soil was 0.27%. The mean particle size of the Lula soil particles used to pack the soil column is about 250 μm. The soil solid density is 2.62 g/cm³. The soil surface area was determined by BET method to be 1.24 m²/g (Micromeritics Instrument Co., Norcross, GA). The porosity of the soil column, determined from the retention volume of tritiated water, was 0.40.

The soil column apparatus was composed primarily of a syringe pump, a soil column and an autosampler. The column is a borosilicate precision glass column (0.9 cm ID, 7 cm L, Spectrum Medical Industries, Inc., Los Angeles, CA) with plungers on both sides of the column. Type 316 stainless steel tubing (1/16" O.D., 0.005" I.D., Small Parts Inc., Miami Lakes, FL) was used to connect the syringe pump with the column and the column with the autosampler. A glass Gastight® syringe with capacity of 50 mL (Hamilton Co., Reno, Nevada) put on the syringe infusion pump (Harvard Apparatus Inc., Holliston, Massachusetts) was used to introduce nano-C₆₀ suspensions or naphthalene solutions to the soil column. The effluent collection was accomplished by an ISCO autosampler (ISCO Inc., Lincoln NE), which was equipped with a Type 316 stainless steel piercing device.

Air dried and sieved soil, 4.9 g, was packed into the glass column to a depth 5 cm. The soil was retained in the column with a 10 μm stainless steel screen positioned at the end of each plunger. 0.01M NaCl/0.01M NaN₃ electrolyte solution was passed through the soil column at a flow rate of 1 mL/hr for about 36 hrs after packing, to ensure compaction and equilibration of soil with the influent solution. Any air bubbles remaining in the soil column were removed by the electrolyte solution.

Nano-C₆₀. C₆₀ solids (purity > 99.5%) were purchased from SES Research (Houston, TX, USA). Input suspensions of nano-C₆₀ were prepared by mixing C₆₀/THF solution with water, followed by removal of THF, as described in a previous paper¹². C₆₀ concentration of the nano-C₆₀ suspension used as the influent in breakthrough

experiments was 48 mg/L. NaCl and NaN₃ solids were dissolved in the nano-C₆₀ suspension to make the concentrations of NaCl and NaN₃ both 0.01M.

Breakthrough Experiments.

1) Nano-C₆₀ breakthrough experiments. The nano-C₆₀ suspension (C₆₀ concentration = 48 mg/L) was initially introduced into the soil column with the syringe pump at different flow rates: 1 mL/hr (linear velocity = 0.38 m/d), 10 mL/hr (linear velocity = 3.8 m/d), and 30 mL/hr (linear velocity = 11.4 m/d). Fractions of the effluent were collected in pre-weighed 8-mL glass vials. Collection time for each sample varied from 0.11 to 2 hrs. After the collection of all samples, glass sample vials were weighed and concentration of nano-C₆₀ in each vial was determined by UV absorbance at 446 nm wavelength on a UV-Vis spectrophotometer (DR/4000, HACH Company, Loveland, CO). The concentration of nano-C₆₀ in the suspension before introducing into the soil column, C₀, and the concentrations of nano-C₆₀ in the effluent, C, were used to obtain a breakthrough curve of C/C₀ as a function of the number of pore volumes.

The pump was shut down for 7 days after the nano-C₆₀ breakthrough experiments. Next, a C₆₀-free electrolyte solution (0.01M NaCl and 0.01M NaN₃) was loaded in a clean glass syringe and pumped into the soil column to further examine the effect of flow rate and flow interruption on the flush-out of nano-C₆₀ particles. Electrolyte solution flow velocities of 0.38, 3.8, 11.4, 15.2 and 22.8 m/d were used. Effluent was collected periodically with 8-mL glass vials following the same procedure as that used for collection of nano-C₆₀ effluent. Concentration of nano-C₆₀ in each collecting vial was also determined by UV absorbance at 446 nm.

2) Naphthalene breakthrough experiments. After conducting the last tracer breakthrough experiments the column was flushed with 0.01M NaCl/0.01M NaN₃ background electrolyte solution at the flow rate of 1 mL/hr for more than 10 hrs until no ³H₂O was detectable in the effluent. Next, naphthalene breakthrough experiments were conducted on the soil column with ¹⁴C-naphthalene aqueous solution (¹⁴C-naphthalene = 0.58 mg/L).

The prepared ¹⁴C-naphthalene aqueous solution was introduced into the soil column with the syringe pump at a flow rate of 1 mL/hr for 45 hrs. The effluent was collected hourly. Glass scintillation vials (with open-top polypropylene closures), each filled with 10 mL of Ready Safe™ scintillation cocktail, were pre-weighed and used for effluent collection. During the sample collection, the delivery end of the tubing pierced through the rubber septa of each glass vial to deliver naphthalene effluents below the cocktail surface in each vial. Effluent naphthalene concentrations were determined with a Beckman liquid-scintillation counter.

After continuous introduction of naphthalene solution for 45 hrs, naphthalene-free electrolyte solutions (0.01M NaCl, 0.01M NaN₃) were introduced into the soil column at the flow rate of 1 mL/hr. The effluent was collected following the same procedure as that used for collection of naphthalene solution and concentrations were measured the same way. The collecting period for each sample varied from 1 hr to 2.5 hrs.

Results and Discussion

Nano-C₆₀ breakthrough experiments.

The deposition kinetics of particles in porous media can be described by the following expression ¹³:

$$\frac{dC}{dL} = -\frac{3}{4}\alpha\eta\frac{(1-\varepsilon)}{a_c}C \quad (1)$$

where C is the particle concentration, L is the particle travel distance in the porous media, a_c is the average radius of the grains comprising the porous media ($a_c = 125 \times 10^{-6}$ m in this study), ε is the porosity of the porous media, η is the single collector efficiency, and α is the particle attachment efficiency. The process of particle deposition can be divided into two sequential steps: the transport of particles from the bulk of the fluid to the vicinity of a stationary surface, and the attachment of particles onto the collector surfaces^{13, 14}. In Eqn. (1), η describes the transport of particles to a single collector; and α describes the attaching efficiency at the collector surface. The product of α and η describes the ratio of the flux of particles actually adhering to a stationary collector to the flux of suspended particles approaching it from upstream.

The single collector efficiency (η) is the ratio of particle flux reaching the collector surface to the particle flux approaching the collector from upstream. It describes the physical effects on the kinetics of particle deposition, and varies with factors such as flow velocity, media porosity, particle and collector diameters, etc. It has been reported that the value of η_{theor} , the theoretical single collector efficiency, can be approximated by the sum of three transport processes that contribute to the particle transport to a collector surface: Brownian diffusion, interception, and gravity forces (sedimentation)¹³⁻¹⁵. Therefore, the value of η_{theor} can be calculated from experimental parameters and a few constants, including particle radius, collector (grain) radius (a_c), particle density, fluid density, porous media porosity (ε), temperature, viscosity of water, superficial or approach velocity of flow (U), gravitational acceleration, Hamaker constant, and Boltzmann's constant¹³⁻¹⁵.

The attachment efficiency α describes the ratio of the total particle deposition rate on a collector to the rate of collisions occurring between suspended particles and the collector. Chemical effects on the particle deposition are usually considered in evaluating the α value. With the value of η_{theor} , the attachment efficiency α can be calculated by integrating Eqn. (1) with boundary conditions that $C = C_0$ at $L = 0$ and $C = C_L$ at $L = L$:

$$\alpha = -\left[\ln\left(\frac{C_L}{C_0}\right) \right] \cdot \left[\frac{4a_c}{3(1-\varepsilon)\eta_{\text{theor}}L} \right] \quad (2)$$

where C_0 and C_L represent particle concentration at $L = 0$ and at $L = L$, respectively.

The particle mobility can be further illustrated by calculating the particle travel distance^{9, 16, 17}. The maximum travel distance (L_T) is defined as the predicted travel distance after which 99.9% of the particles are immobilized by the porous media. It can be calculated by rearranging Eqn. (2) and using 0.001 as the value for (C_L/C_0) .

Figure 1 shows the breakthrough curves of nano- C_{60} particles at different flow rates: 1 mL/hr (linear flow velocity = 0.38 m/d), 10 mL/hr (linear flow velocity = 3.8 m/d), and 30 mL/hr (linear flow velocity = 11.4 m/d). On the graph, the x-axis represents the numbers of pore volumes of nano- C_{60} suspension that have passed through the soil column. The y-axis is the ratio of the nano- C_{60} concentration exiting the column (C , mg/L), and the nano- C_{60} concentration in the input (C_0 , mg/L). Nano- C_{60} particles were

first observed in the effluent after about 3.2 pore volumes. The concentration of nano-C₆₀ particles increased gradually until it reached a peak value of 47% at about 53.5 pore volumes. Interestingly, after that, the fraction of influent nano-C₆₀ particles exiting the column decreased sharply from 47% to 0% in only about 3 pore volumes. The introduction of nano-C₆₀ particles was continued for another 60 pore volumes and virtually no nano-C₆₀ particles passed through the soil column in the last 60 pore volumes, as shown in Figure 1. This “favorable deposition” ($\alpha = 1$) possibly indicated an irreversible sorption of the nano-C₆₀ particles on the soil column. This may be related to the phenomenon of “filter ripening”, a process known in packed-bed filtration¹⁴. Particles that are deposited from a flowing suspension at one time can then become filter media for subsequent particles that are traveling in the pores of the media. Although further study is necessary to better understand the mechanisms underlying this observed “favorable deposition”, it was observed repeatedly in the current study under the low flow rate condition (1 mL/hr, or linear velocity of 0.38 m/d, Figure 1) and may have broad environmental significance.

Following a period of a 72 hour shut-in, the flow was resumed and the flow rate was changed to 10 mL/hr. The value of C/C_0 is about 0.63 after about 4.4 pore volumes, which is about 3 times that of nano-C₆₀ passage at flow rate of 1 mL/hr. The plateau value of nano-C₆₀ passage through the soil column at flow rate of 10 mL/hr was observed to be $60 \pm 3\%$. The flow rates were then changed to 30 mL/hr, 10 mL/hr, and 1 mL/hr. At 30 mL/hr $C/C_0 \approx 0.73$ after 3.9 pore volumes and remained relatively constant for the following 8 pore volumes. Interestingly, when the flow rates were suddenly changed from 30 mL/hr to 10 mL/hr, and from 10 mL/hr to 1 mL/hr, spiked release of nano-C₆₀ particles was observed, with $C/C_0 = 0.86$ and 0.95 , respectively.

Next, following another 72-hour shut-in, the flow of nano-C₆₀ particles was resumed at 1 mL/hr for 18 pore volumes then 10 mL/hr for 8 pore volumes and finally 30 mL/hr for 24 pore volumes, all without interruption or shut-in. At the flow rate of 1 mL/hr, the percent of nano-C₆₀ breakthrough reached a peak value of 95% in the first 1.6 pore volumes, and that value dropped dramatically to 2.5% at 9.4 pore volumes. The C/C_0 value fluctuated slightly around zero but did not exceed 1% in the following 9 pore volumes. This observation was consistent with the first part of this graph (flow rate = 1 mL/hr), where no nano-C₆₀ passed through the soil column after about 56.7 pore volumes. The unexpectedly high C/C_0 value at 1.6 pore volumes ($C/C_0 = 0.95$) for the 1 mL/hr flow rate is probably due to the flow interruption (3 days) before that. A similar spike of nano-C₆₀ following flow interruption and velocity change was observed in nano-C₆₀ flush-out experiments with nano-C₆₀-free electrolyte solution and will be discussed in a later section. As shown in Figure 1, when the flow rate was changed from 1 mL/hr to 10 mL/hr after about 18 pore volumes, nano-C₆₀ particles started to pass through the soil column and the percentage of passage reached 59% in 2.6 pore volumes. Then, the flow rate was increased to 30 mL/hr at 26 pore volumes and the plateau value of nano-C₆₀ passage was $\sim 80\%$. Finally, the flow rate was changed back to 10 mL/hr, and a spike release of nano-C₆₀ particles with $C/C_0 = 1.17$ was also observed, similar to what was observed earlier when flow rates were changed from higher to lower.

The values of the theoretical single collector efficiency (η_{theor}) was calculated using an online calculator at: www.colorado.edu/ceae/environmental/ryan/cven6414/eta.xls^{13, 15} and listed in Table 1.

It should be noted that at the particle size range of nano-C₆₀ particles (~100 nm), the Brownian diffusion is the dominant process in the particle transport to the collector surface. The effect of direct interception and gravity forces on the particle transport is negligible. The corresponding α values were then calculated using Eqn. (2) and listed in Table 1.

It can be seen from comparing the values in Table 1 that the value of $\alpha \cdot \eta_{\text{theor}}$ decreases with increasing flow velocity, meaning that the deposition of nano-C₆₀ particles are favored at lower flow rates, i.e., nano-C₆₀ particles are more mobile at higher flow rates. Consequently, the maximum travel distance to remove 99.9% of nano-C₆₀ particles to the porous media increased with increasing flow velocity. For example, at the flow rate of 1 mL/hr, nano-C₆₀ particles could travel only 31 cm before 99.9% of the particles were removed by the soil column, while at the flow rate of 30 mL/hr, nano-C₆₀ particles could travel 1.32 m before 99.9% of the particles were removed by the soil column.

Results for nano-C₆₀ particle flush-out experiments, initiated 7 days after the completion of nano-C₆₀ breakthrough experiments, are shown in Figure 2. $C_0 = 48$ mg/L is assumed in each case. Initial flow rate used was 10 mL/hr. A peak of nano-C₆₀ ($C/C_0 = 0.46$) was apparently reached at 2 pore volumes. After 4 pore volumes, no further nano-C₆₀ breakthrough was observed, despite the fact that the flow rate was increased to 30 mL/hr without interruption at 13.8 pore volumes. The second nano-C₆₀ flush-out experiment was conducted after 3 days of shut-in. Initial flow rate used in this experiment was 30 mL/hr. A peak of nano-C₆₀ passage, $C/C_0 = 0.13$, was reached at 5.9 pore volumes. After that, the value of C/C_0 for nano-C₆₀ particles dropped to zero, despite the fact that the flow rate was increased to 40 and then 60 mL/hr at 71 and 181 pore volumes, respectively. The last nano-C₆₀ flush-out experiment was conducted 3 days after the second set. A single flow rate of 1 mL/hr was used. The value of C/C_0 for nano-C₆₀ reached a peak value of 107% at 1.6 pore volumes, and then decreased gradually to zero after 7.9 pore volumes. No nano-C₆₀ breakthrough was observed thereafter.

Naphthalene breakthrough experiments.

The transport of contaminants in soil columns is generally described by a one dimensional advective-dispersion equation (ADE)¹⁸:

$$R \frac{\partial C}{\partial T} = D \frac{\partial^2 C}{\partial x^2} - v \frac{\partial C}{\partial x} \quad (3)$$

where C represents contaminant concentration in the flowing water; T and x are the contaminant travel time and travel distance; and v represents the linear flow velocity. R in Eq. 2 denotes the retardation factor:

$$R = 1 + (\rho_b / \varepsilon)(dq/dC) \quad (4)$$

where ρ_b is the bulk density of the porous media; ε is media porosity; and q is the amount of contaminant sorbed on the porous media (e.g. soil) per gram of solid weight. If $q = K_p C$ (a linear isotherm) then $dq/dC = K_p$ and K_p can be calculated from measured values of R .

After the completion of all nano-C₆₀ breakthrough experiments, the mass of C₆₀ retained on this soil column was calculated to be about 1.8 mg-C₆₀/g-soil, i.e., 0.18% of soil mass. ¹⁴C labeled naphthalene aqueous solution (¹⁴C-naphthalene = 0.58 mg/L) was passed through this soil column at the flow rate of 1 mL/hr for 45 hrs, followed by flushing with naphthalene-free electrolyte solution. Data are shown in Figure 3 (curve c).

Curve a is the tracer ($^3\text{H}_2\text{O}$) breakthrough curve for this soil column. Naphthalene transport through the same soil has been studied by Kan and Tomson¹⁹ with a different column using the same packing method. The naphthalene breakthrough curve is included Figure 3 (curve b) for comparison.

It can be seen from Figure 3 that in the breakthrough experiment with the column in this study (Lula soil with 0.18% of nano- C_{60} , curve c), only 10% of naphthalene passed through the column at 5.3 pore volumes, which is 24% of the C/C_0 value on curve b, at the same number of pore volumes. At 34.1 pore volumes, C/C_0 for naphthalene reached the peak value of 0.89 in the Lula/0.18% nano- C_{60} column, while C/C_0 for naphthalene in the Lula soil only column reached 98.5% in only 13.9 pore volumes. In the naphthalene flush-out experiment following 34.1 pore volumes of continuous introduction of naphthalene solution, the C/C_0 value of naphthalene dropped to 14% at 68.2 pore volumes. During the next 37.8 pore volumes, the C/C_0 value for naphthalene dropped from 14% to 1.4%.

The partition coefficient of naphthalene with Lula soil was reported to be $K_{\text{soil}} = 1.91 \text{ mL/g}$ ¹⁹ i.e., $K_{\text{oc}} = K_{\text{soil}} / f_{\text{oc}} = 1.91 / 0.0027 = 707 \text{ mL/g}$. Using this value and the porosity of 0.40 and the bulk density of 1.57 g/cm^3 for Lula soil, a retardation factor $R = 8.5$ can be calculated for breakthrough curve b (Figure 3) with Eqn. (4). The retardation factor (denoted as R') for the naphthalene breakthrough curve with the Lula/0.18% nano- C_{60} column (curve c in Figure 3) is about 13.1 at $C/C_0 = 0.5$. The soil partition coefficient for naphthalene with Lula/0.18% nano- C_{60} can be calculated from this R' value with Eq. 3, $K_{\text{soil}, 0.18\% \text{C}_{60}} = 3.08 \text{ mL/g}$. Therefore, the organic carbon normalized partition coefficient for naphthalene with the nano- C_{60} on Lula soil column is calculated to be $K_{\text{oc}} = 10^{2.81} \text{ mL/g}$. This K_{oc} value is similar to the K_{oc} value obtained for naphthalene with Lula soil ($10^{2.85} \text{ mL/g}$). It is therefore can be seen that the effect of 0.18% adsorbed nano- C_{60} particles in the soil column on naphthalene transport is similar to that of 0.18% soil organic carbon.

Conclusions

Although C_{60} was expected to be very hydrophobic, water-stable nano- C_{60} particles could be produced by simple methods without any surface treatments⁴⁻⁶. This increased apparent hydrophilicity may lower the attachment efficiency of nano- C_{60} particles and consequently increase the mobility of C_{60} . If this is true, the public may be more concerned about the exposure to the mobilized C_{60} , since there are already studies showing the toxicity of nano- C_{60} to fish and to cultured human cells^{1,2}.

However, it may be concluded from this study that at the typical groundwater flow rate ($\sim 1 \text{ ml/hr}$ in this study), nano- C_{60} particles showed very limited mobility: nano- C_{60} particles breakthrough did not reach 100% and all nano- C_{60} particles were immobilized by the soil column after a few pore volumes. Nano- C_{60} particles showed higher mobility at increased flow rates. Spiked release of nano- C_{60} particles was observed after flow interruption and flow velocity changes, indicating that unexpected release of nano- C_{60} particles might occur under complex aqueous environments. The adsorbed nano- C_{60} particles in the soil column affected naphthalene transport similarly to soil organic carbon.

Acknowledgements

We gratefully acknowledge Dr. Wenhua Guo at Rice University for running the TEM and Professor Mark Wiesner for help with particle size measurements. The financial supports of the National Science Foundation through the Center for Biological and Environmental Nanotechnology [EEC-0118007], U.S. EPA ORD/NCER/STAR nanotechnology program, U.S. EPA Hazardous Substance Research Center/South & Southwest Region, and Rice University Brine Chemistry Consortium of companies: Aramco, Baker-Petrolite, Champion Technologies, Inc., Chevron-Texaco, Inc., Clariant UK Ltd., ConocoPhillips, Inc., Marathon Oil, Nalco, Occidental Oil and Gas, are greatly appreciated.

References:

1. E. Oberdorster: Manufactured nanomaterials (fullerenes, C₆₀) induce oxidative stress in the brain of juvenile largemouth bass. *Environ. Health Perspect.* **112** (10), 1058-1062 (2004).
2. C.M. Sayes, J.D. Fortner, W. Guo, D. Lyon, A.M. Boyd, K.D. Ausman, Y.J. Tao, B. Sitharaman, L.J. Wilson, J.B. Hughes, J.L. West and V.L. Colvin: The differential cytotoxicity of water-soluble fullerenes. *Nano Lett.* **4** (10), 1881-1887 (2004).
3. R.S. Ruoff, D.S. Tse, R. Malhotra and D.C. Lorents: Solubility of fullerene (C₆₀) in a variety of solvents. *J. Phys. Chem.* **97** (13), 3379-3383 (1993).
4. W.A. Scrivens, J.M. Tour, K.E. Creek and L. Pirisi: Synthesis of ¹⁴C-labeled C₆₀, its suspension in water, and its uptake by human keratinocytes. *J. Am. Chem. Soc.* **116**, 4517-4518 (1994).
5. G.V. Andrievsky, M.V. Kosevich, O.M. Vovk, V.S. Shelkovsky and L.A. Vashchenko: On the production of an aqueous colloidal solution of fullerenes. *J. Chem. Soc. Chem. Commun.* **12**, 1281-1282 (1995).
6. S. Deguchi, R.G. Alargova and K. Tsujii: Stable Dispersions of Fullerenes, C₆₀ and C₇₀, in water. Preparation and characterization. *Langmuir* **17** (19), 6013-6017 (2001).
7. X. Cheng, A.T. Kan and M.B. Tomson: Naphthalene adsorption and desorption from aqueous C₆₀ fullerene. *J. Chem. Eng. Data* **49**, 675-683 (2004).
8. A.T. Kan and M.B. Tomson: Ground Water Transport of Hydrophobic Organic Compounds in the Presence of Dissolved Organic Matter. *Environ. Toxicol. Chem.* **9**, 253-263 (1990).
9. H.F. Lecoanet, J. Bottero and M.R. Wiesner: Laboratory assessment of the mobility of nanomaterials in porous media. *Environ. Sci. Technol.* **38**, 5164-5169 (2004).
10. H.F. Lecoanet and M.R. Wiesner: Velocity effects on fullerene and oxide nanoparticle deposition in porous media. *Environ. Sci. Technol.* **38**, 4377-4382 (2004).
11. J.T. Wilson, C.G. Enfield, W.J. Dunlap, R.L. Cosby, D.A. Foster and L.B. Baskin: Transport and fate of selected organic pollutants in a sandy soil. *J. Environ. Qual.* **10**, 501-506 (1981).
12. X. Cheng, A.T. Kan and M.B. Tomson: Uptake and sequestration of naphthalene and 1,2-dichlorobenzene by C₆₀. *J. Nanoparticle Res.* **7**, 555-567 (2005).

13. K.M. Yao, M.T. Habibian and C.R. O'Melia: Water and wastewater filtration: concepts and applications. *Environ. Sci. Technol.* **5**, 1105-1112 (1971).
14. C.R. O'Melia: Kinetics of colloid chemical processes in aquatic systems., in *Aquatic Chemical Kinetics--Reaction Rates of Processes in Natural Waters*, edited by W. Stumm, Editor. (John Wiley & Sons, Inc.: New York. 1990), p. 447-474.
15. R. Rajagopalan and C. Tien: Trajectory analysis of deep-bed filtration with the sphere-in-cell porous media model. *Am. Inst. Chem. Eng. J.* **22**, 523-533 (1976).
16. M. Elimelech, J. Gregory, X. Jia and R.A. Williams: Particle Deposition and Aggregation. Measurement, Modeling, and Simulation. (Butterworth-Heinemann, Woburn, MA, 1995).
17. R. Kretzschmar and H. Sticher: Transport of humic-coated iron oxide colloids in a sandy soil: influence of Ca²⁺ and trace metals. *Environ. Sci. Technol.* **31**, 3497-3504 (1997).
18. J. Bear: *Hydraulics of Groundwater*. (McGraw-Hill, New York, NY, 1979).
19. A.T. Kan and M.B. Tomson: Effect of pH concentration on the transport of naphthalene in saturated aquifer media. *J. Contam. Hydrol.* **5** (3), 235-251 (1990).

Table 1. Parameters for nano-C₆₀ particles transport in Lula soil column. v (m/d) – linear flow velocity; U (m/d) – superficial or approach velocity; η_{theor} – theoretical single collector efficiency; α – particle attachment efficiency; L_T (m) – the distance at which 99.9% of nano-C₆₀ particles ($C_L/C_0 = 0.001$) are removed by the porous media.

flow rate (mL/hr)	v (m/d)	U (m/d)	η_{theor}	C/C₀	α	$\alpha \cdot \eta_{\text{theor}}$	L_T (m)
1 (0-56.5 PV) ^a	0.38	0.152	1.35	0.33±0.07	0.0046	0.0062	0.31
1 (56.5-116.5PV) ^b	0.38	0.152	1.35	0	1	—	—
10	3.8	1.52	0.29	0.60±0.03	0.0098	0.0028	0.68
30	11.4	4.56	0.14	0.77±0.04	0.0104	0.0015	1.32

^avalues in this line were calculated from 1 mL/hr breakthrough data from 0 to 56.5 pore volumes; ^bvalues in this line were calculated from 1 mL/hr breakthrough data from 56.5 to 116.5 pore volumes.

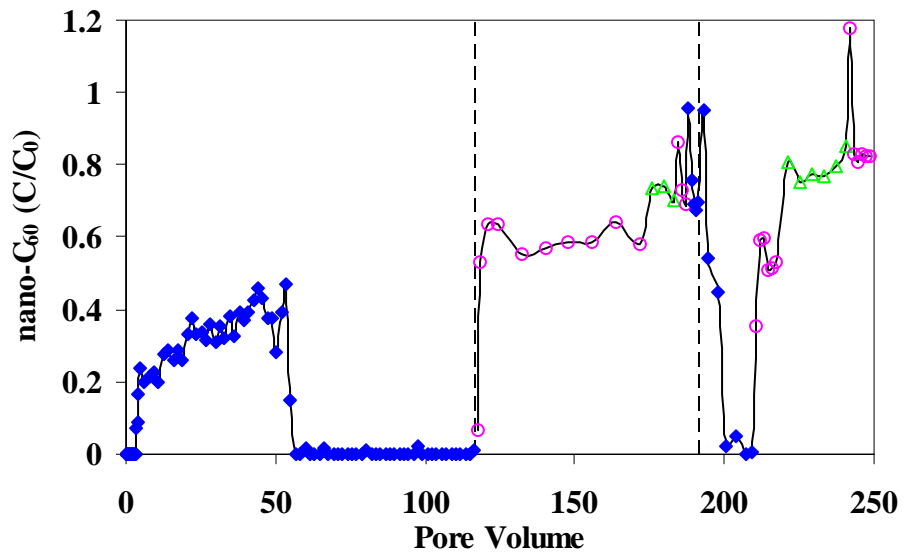


Figure 1. Nano- C_{60} breakthrough curves at different flow rates. \blacklozenge , flow rate is 1 mL/hr ($v = 0.38$ m/d); \circ , flow rate is 10 mL/hr ($v = 3.8$ m/d); \triangle , flow rate is 30 mL/hr ($v = 11.4$ m/d). ----: flow interruption is 3 days.

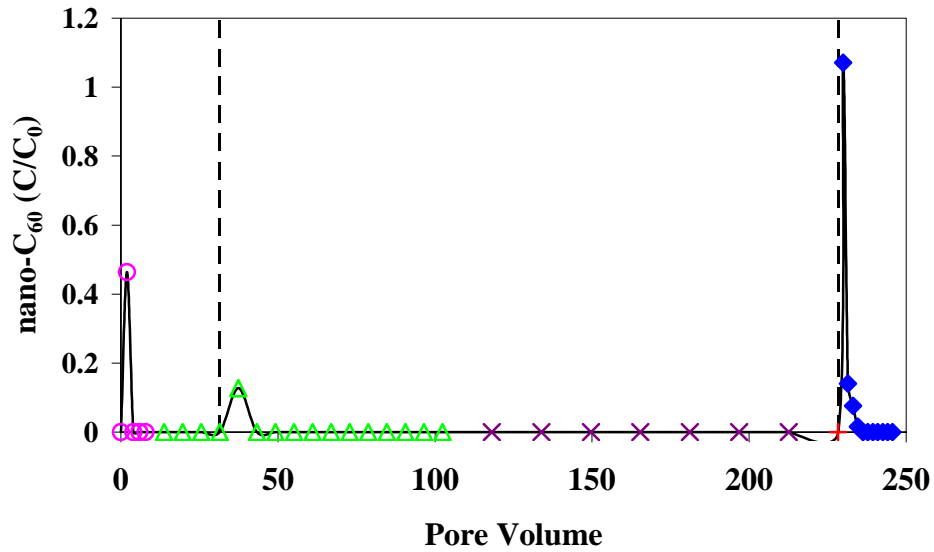


Figure 2. Plots of percentage of nano-C₆₀ passage through the soil column versus pore volume during the nano-C₆₀ flush-out experiments. ♦, flow rate is 1 mL/hr ($v = 0.38$ m/d); o, flow rate is 10 mL/hr ($v = 3.8$ m/d); Δ, flow rate is 30 mL/hr ($v = 11.4$ m/d). ×, flow rate is 40 mL/hr ($v = 15.2$ m/d); +, flow rate is 60 mL/hr ($v = 22.8$ m/d); ----: flow interruption is 3 days.

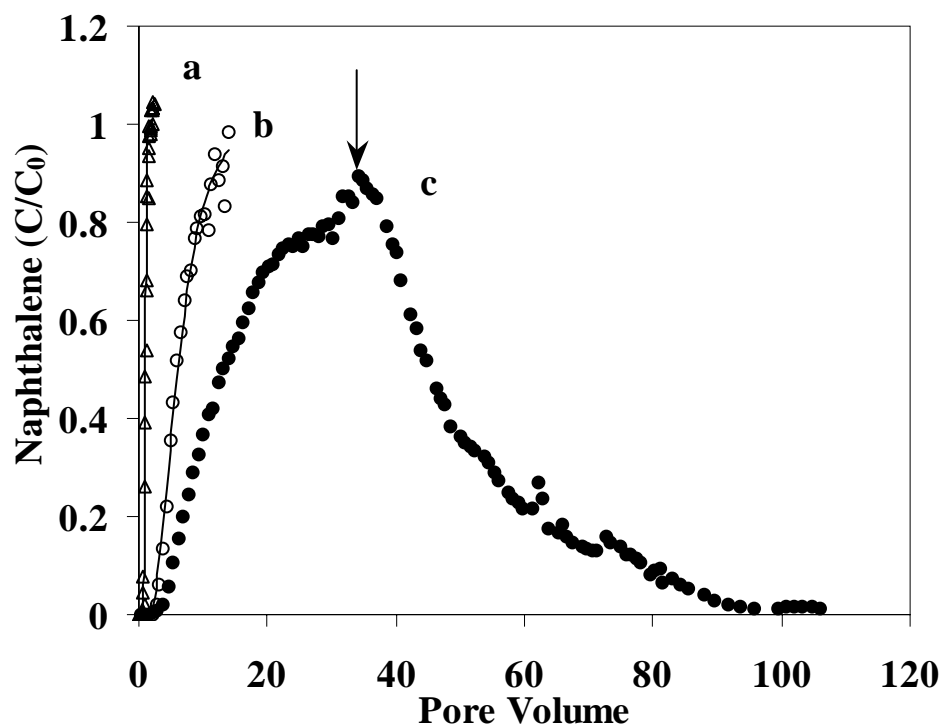


Figure 3. a. Tracer ($^3\text{H}_2\text{O}$) breakthrough curve. b. naphthalene breakthrough curve from Lula soil column. c. naphthalene breakthrough curve from Lula soil column with 0.18% of nano- C_{60} particles deposited.